

# Full-Wave Analysis and Optimization of a TARA-Like Shield-Assisted Paraboloidal Reflector Antenna Using a Nystrom-Type Method

Vitaliy S. Bulygin, *Member, IEEE*, Trevor M. Benson, *Senior Member, IEEE*, Yuriy V. Gandel, *Senior Member, IEEE*, and Alexander I. Nosich, *Fellow, IEEE*

**Abstract**—Using the recently developed method based on the rigorous theory of singular and hypersingular integral equations (IEs) and Nystrom-type discretization, a paraboloidal reflector assisted with a conical shield is investigated. To decrease the computation time we propose a new method of calculation of the Modal Green's Functions in the quasi-optical range. The far and near fields of the studied reflector are analyzed in the transmission and reception cases, and reveal fine features that escape asymptotic analysis. Elementary numerical optimization of the shield-assisted paraboloidal antenna is performed.

**Index Terms**—Body of revolution (BOR), complex Huygens element, conical shield, directivity, focusing, integral equation, modal Green's function, reflector antenna.

## I. INTRODUCTION

TRANSPORTABLE atmospheric radar (TARA) is a real system used at the Delft University of Technology for studying atmospheric phenomena such as clouds, precipitations and clear air turbulence [1], [2]. It has two antennas mounted on a common platform. Each antenna is a combination of a paraboloidal reflector and a conical shield, and can be viewed as a two-reflector antenna where reflectors are welded together along the rim of the paraboloid. The aim of such a design is to reduce the signals received from all directions below the plane of the paraboloid rim to  $-70$  dB and lower, because normally TARA looks into the zenith and only the signals reflected from that direction are relevant.

The radiation pattern of the full TARA system has been successfully simulated in [2], [3] using the electric-field integral equation (EFIE) solved using the multilevel-fast-multipole or modified method-of-moments algorithm (MLFMP-MM) with

the Rao-Wilton-Glisson (RWG) basis functions [4]. In addition to the reflector, the authors of [2], [3] took into account the presence of struts and feed housings. As a result, they did not exploit the rotational symmetry of reflector itself and therefore had to deal with large-size matrices. From the modelling point of view more stressful is the fact that the convergence of MLFMP-MM has not been proven mathematically.

The IE-based methods have been used in the numerical modeling of three-dimensional (3-D) electromagnetic wave diffraction by arbitrary PEC screens (i.e. finite zero-thickness surfaces) since long ago [4], [5]. Here, rotationally symmetric PEC screens occupy a special place. This is because the symmetry can be taken into account analytically, and the 3-D problem can be reduced to an infinite set of 1-D IEs for the independent azimuthal harmonics that significantly decreases the order of the final matrices. The papers [6]–[8] have been instrumental in the analysis of such screens and other rotationally symmetric scatterers.

Discretization plays a very important role in the numerical solutions of IEs. In the present paper the same problem as in [2], [3] is numerically studied using a Nystrom-type meshless discretization. This means that the unknown smooth function is approximated by a polynomial of high enough order and interpolation-type quadrature formulas with theoretically proven convergence are used to compute the integrals. In 2-D, this technique has been successfully used in [9]–[12] to analyze the scattering and focusing by single and multiple PEC and imperfect screens. The 3-D case is more complicated however recently we have developed a corresponding algorithm [13], [14] that exploits rotational symmetry, leads to small matrices, and has guaranteed convergence. As all basic equations of these works are valid for arbitrary PEC screens with rotational symmetry, we will not present them here and, instead, make necessary references. We will therefore emphasize numerical results obtained with this accurate method in the analysis of the TARA reflector antenna.

The separation of the azimuth harmonics shifts the computation time expenditures to the calculation of the modal Green's function (MGF) [15]–[23]. Each of these papers presented a way to calculate the MGF in a certain domain of parameters. However all these methods depend on the electrical size of the scatterer contour and lose efficiency and accuracy if this size increases. In the quasi-optical case the MGF is an integral with a rapidly oscillating integrand and therefore these methods work slowly. Derivation of a formula which does not depend

Manuscript received May 18, 2012; revised February 04, 2013 and June 03, 2013; accepted July 22, 2013. Date of publication July 30, 2013; date of current version October 02, 2013. This work was supported in part by the National Academy of Science of Ukraine and in part by the European Science Foundation via the Networking Programme “Newfocus.”

V. S. Bulygin and A. I. Nosich are with the Laboratory of Micro and Nano Optics, Institute of Radio-Physics and Electronics NASU, Kharkiv 61085, Ukraine (e-mail: Vitaliy\_Bulygin@iee.org).

T. M. Benson is with the George Green Institute for Electromagnetics Research, The University of Nottingham, Nottingham NG7 2RD, U.K.

Y. V. Gandel is with the Department of Mathematical Physics and Computational Mathematics, Kharkiv National University, Kharkiv 61077, Ukraine.

Color versions of one or more of the figures in this paper are available online at <http://ieeexplore.ieee.org>.

Digital Object Identifier 10.1109/TAP.2013.2275248

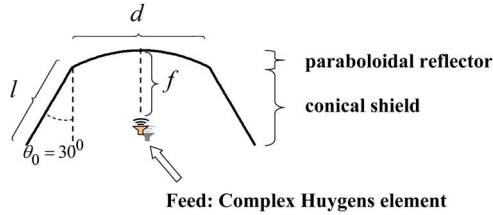


Fig. 1. The cross-section geometry of the TARA-like reflector and CHE feed.

on the electrical size of reflector and has exponential convergence is crucial for the accurate analysis of the TARA and any other large-size reflector far-field and near-field on a personal computer.

The problem formulation is presented in Section II. In Section III, we model the feed using a complex Huygens element (CHE). In Section IV, we derive a series representation for the calculation of MGF. Section V is dedicated to an investigation of the near and far fields of the TARA-like reflector in the transmission (CHE-fed) and on-axis reception (plane-wave fed) cases. Conclusions are summarized in Section VI. Time dependence is  $\exp(i\omega t)$  and  $k = \omega/c$  is the wavenumber ( $c$  being the light velocity).

## II. PROBLEM FORMULATION

Fig. 1 shows the cross-sectional geometry of the TARA-like antenna without struts and feed housings. The working wavelength is supposed to be  $\lambda = 9.1$  cm. The main paraboloidal reflector has a diameter  $d$  of 3 meters or  $33\lambda$  and its focal distance is  $f = 0.5d$ . The shield has a width  $l$  of 2 meters or  $22\lambda$  and an angle of inclination  $\theta_0 = 30^\circ$ .

As usual, we consider the total field to be a sum of the incident and scattered fields,  $\vec{E}^{tot} = \vec{E} + \vec{E}^0$ . For unique determination of the unknown scattered field, it must satisfy Maxwell's equations outside the reflector, the Sommerfeld radiation condition, the Meixner edge condition, and the PEC boundary condition on the surface of the reflector. For modelling the TARA in the transmission case, the feed will be simulated using a CHE placed at the geometrical focus of the paraboloidal part of reflector (see Section III). For modelling the TARA in the reception case, we will consider the incident field as a plane electromagnetic wave propagating along the axis of the reflector.

Exploiting the rotational symmetry of the TARA reflector, we represent the unknown current density as a Fourier series in the azimuth angle  $\psi$ :  $\vec{j}(t, \psi) = \sum_{M=-\infty}^{\infty} \vec{j}^M(t) e^{iM\psi}$ , where  $t$  is the parameter of a rotational contour parameterization. In [12]–[14] the diffraction by a PEC axially symmetric screen has been reduced, for each  $M$ -th azimuthal harmonic of the current density components, to two coupled 1-D IEs with varying coefficients. One of these IEs is hypersingular and the other is singular. Their meshless discretization is based on the Nystrom-type scheme and specifically tailored quadrature formulas of interpolation type [10], [11], [24]–[26]. This method has guaranteed (mathematically proven) convergence for arbitrary frequency and other parameters, i.e. in the full range from statics via resonance range to quasi-optics. The rate of convergence is very fast if the order of interpolation is larger than the electrical length of reflector's cross-sectional contour (length

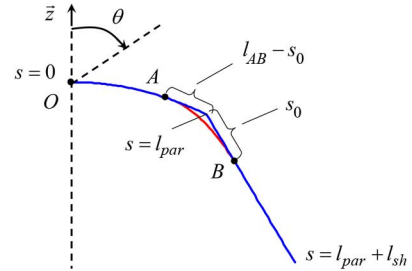


Fig. 2. Smoothing of the shield-assisted paraboloidal reflector contour.

times wavenumber). From the solutions of these IEs the surface current and the scattered field are obtained.

However, if the reflector size lies in the quasi-optical range the method of [12]–[14] can be improved even further to provide faster computations. These improvements relate to the calculation of MGFs and will be considered in Section IV.

Besides, the rate of convergence of the method considered strongly depends on the contour smoothness. The contour of the TARA reflector has a bend between the parabola and the straight interval corresponding to the shield. Suppose that  $\rho(s), z(s)$  is the *natural* parameterization of the shield-assisted paraboloidal screen contour (the expressions of this parameterization have been established), where  $s$  is the arc length counted from the paraboloid vortex. Denote also the parabolic-part length as  $l_{Par}$  and the shield-part length as  $l_{Sh}$ . Now, fix the points  $A$  and  $B$  on the rotation contour, so that the parameter corresponding to  $A$  ( $B$ ) is smaller (larger) than the parameter corresponding to the bend point (Fig. 2).

Suppose that  $l_{AB}$  is the contour length between the points  $A$  and  $B$ . Then the parameter value  $l_A = l_{Par} + s_0 - l_{AB}$ ,  $s_0 \in (0, l_{AB})$  corresponds to the point  $A$  and the parameter value  $l_B = l_{Par} + s_0$ ,  $s_0 \in (0, l_{AB})$  corresponds to the point  $B$ . To approximate the bend between points  $A$  and  $B$ , one can use a spline. There is a set of splines with two parameters,  $s_0$  that is the distance from  $B$  to the bend point and  $l_{AB}$  that is the length of interpolated arc. We have chosen the spline with the smallest length as a function of  $s_0$ . If  $l_{AB}$  is smaller, then our spline is nearer to the bend. Our numerical experiments for the TARA-like reflectors have shown that the values of  $l_{AB} = \lambda$  and smaller provide  $10^{-3}$  relative difference in the far field. Therefore we below consider the shield-assisted paraboloidal reflector with a smoothed bend characterized by  $l_{AB} = \lambda$ .

## III. MODELLING THE FEED

When modeling the TARA antenna in the transmission case we assume that the feed is a Complex Huygens Element (CHE). The CHE is a convenient simplified model of a realistic circular corrugated-horn or horn-lens antenna. Its field function depends on the parameter “ $b$ ” that is formally the imaginary part of the source location point. If  $b = 0$  then the field function coincides with the field of the classical Huygens Element (HE) which consists of elementary electric and magnetic dipoles placed orthogonal to each other. As known, the HE has fixed far-zone directivity equal to 3. If  $b$  is increased, then the directivity of such a modified source can be made larger both in the far and near zone, and, correspondingly, the reflector edge illumination can

be lowered. Therefore such a feed is convenient for simulating the incident fields in the modeling of reflector antennas.

Consider the electric field of a CHE placed on the  $z$  axis and shifted by the distance  $z_0$  along the  $z$ -axis.  $\vec{E}^{CHE} = \vec{E}^{CED} + \vec{E}^{CMD}$ , where  $\vec{E}^{CED}$  ( $\vec{E}^{CMD}$ ) is the electric field of a complex electric (magnetic) dipole oriented in parallel to the  $x$ ( $y$ ) axis. The field components are found explicitly as

$$E_{\rho}^{CED} = \frac{e^{-ikR}}{R} \frac{i}{k} \cos \varphi \left[ (\cos^2 \theta - 2 \sin^2 \theta) \left( \frac{1}{R^2} + \frac{ik}{R} \right) - k^2 \cos^2 \theta \right] \quad (1)$$

$$E_{\varphi}^{CED} = -\frac{i}{k} \frac{e^{-ikR}}{R} \sin \varphi \left( \frac{1}{R^2} + \frac{ik}{R} - k^2 \right) \quad (2)$$

$$E_z^{CED} = -\frac{e^{-ikR}}{R} \frac{i}{k} \cos \varphi \sin \theta \cos \theta \left( \frac{3}{R^2} + \frac{3ik}{R} - k^2 \right) \quad (3)$$

$$E_{\rho}^{CMD} = -\left( \frac{e^{-ikR}}{R} \right) \cos \theta \cos \varphi (1/R + ik) \quad (4)$$

$$E_{\varphi}^{CMD} = \left( \frac{e^{-ikR}}{R} \right) \cos \theta \sin \varphi (1/R + ik) \quad (5)$$

$$E_z^{CMD} = \left( \frac{e^{-ikR}}{R} \right) \sin \theta \cos \varphi (1/R + ik) \quad (6)$$

where  $R = [\rho^2 + (z - z_0 - ib)^2]^{1/2}$ ,  $b \geq 0$ . This field function satisfies Maxwell equations exactly and has a circle of branch points at  $z = z_0$ ,  $\rho = b$ ,  $\varphi \in [0, 2\pi]$ , which can be conveniently considered to represent the aperture rim of the real horn.

The far-field pattern of such a feed is introduced as  $\vec{F}(\theta, \varphi) = \lim_{R \rightarrow \infty} \vec{E}(R, \theta, \varphi) R e^{ikR}$  and its components are

$$F_{\varphi}^{CED} = ik \sin \varphi \cdot \exp[-ik \cos \theta (ib - z_0)] \quad (7)$$

$$F_{\varphi}^{CMD} = ik \cos \theta \sin \varphi \cdot \exp[-ik \cos \theta (ib - z_0)] \quad (8)$$

$$F_{\theta}^{CED} = -ik \cos \varphi \cos \theta \cdot \exp[-ik \cos \theta (ib - z_0)] \quad (9)$$

$$F_{\varphi}^{CMD} = -ik \cos \varphi \cdot \exp[-ik \cos \theta (ib - z_0)]. \quad (10)$$

As we can see from (1)–(10), the CHE field has only two Fourier components, with  $M = 1$  and  $M = -1$ . However, one needs to calculate only one component of the current, because  $j_{\tau}^{(1)}(t) = j_{\tau}^{(-1)}(t)$ ,  $j_{\varphi}^{(1)}(t) = -j_{\varphi}^{(-1)}(t)$ , see [12]–[14] for details.

In Fig. 3, we show the dependence of the directivity,  $D = 4\pi |F^{tot}(\pi, 0)|^2 P^{-1}$ ,  $P = \int_S |F^{tot}(\theta, \varphi)|^2 dS$  of a TARA-size paraboloidal reflector without a shield illuminated by the in-focus CHE versus the CHE aperture parameter  $kb$ . One can see that the optimal value  $kb = 2.37$  corresponds to the edge illumination of  $-5.619$  dB. We use a CHE with this optimal parameter in the study of all further configurations.

Fig. 4 shows the far-zone radiation patterns in the E- and H-planes of the TARA parabolic reflector without a conical shield when it is illuminated by the optimal CHE and by the classical HE ( $b = 0$ ). As visible, illumination by CHE provides much lower sidelobes, thanks to lower edge illumination.

In Fig. 5, we visualize, on the logarithmic scale, the near-zone E-field in the E- and H-planes of the paraboloidal reflector illuminated by the HE.

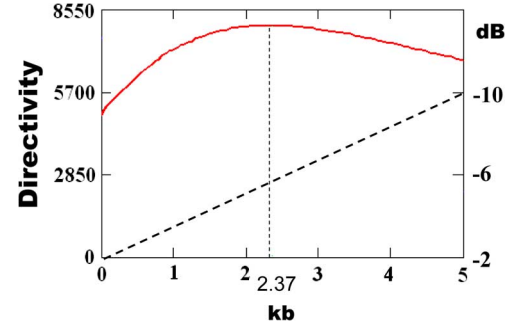


Fig. 3. The directivity of a stand-alone paraboloidal reflector illuminated by CHE as a function of the aperture size parameter (solid line) and the edge illumination (dashed-line).

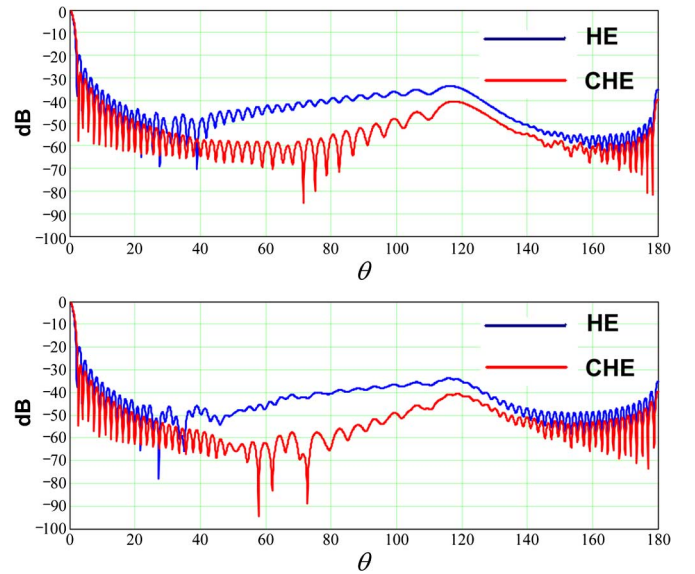


Fig. 4. The total far-zone radiation patterns in the H-plane (top) and the E-plane (bottom) of bare paraboloidal reflector illuminated with the in-focus HE and the CHE with the optimal aperture parameter.

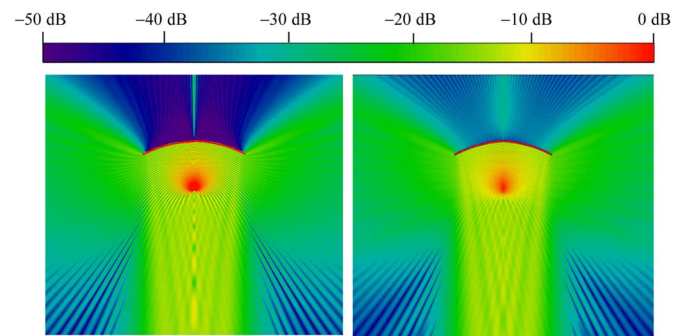


Fig. 5. The near field of the paraboloid illuminated by a HE for  $f = d/2$  and  $d = 33\lambda$  in the H-plane (left) and the E-plane (right).

For comparison, in Fig. 6 we visualize the near-zone E-field of the paraboloidal reflector illuminated by the optimal CHE in the E and H-planes.

The near-field patterns show, in agreement with the far-field pattern, that the use of the optimized CHE instead of a HE lowers the edge illumination and consequently dampens the sidelobes, including the spillover sidelobe.

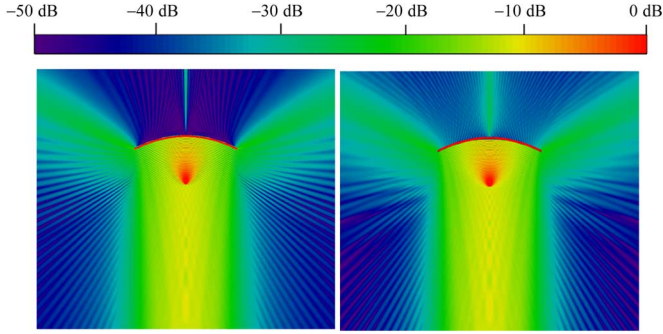


Fig. 6. The same as in Fig. 5 for the paraboloid illuminated by a CHE with the optimal aperture-size parameter  $kb = 2.37$ .

#### IV. CALCULATION OF MGF IN THE QUASI-OPTICAL RANGE

In the quasi-optical range of  $d \gg \lambda$  the unknown current densities have many oscillations on the reflector surface. This calls for high order discretizations of our IEs. Moreover, below we present the results of a partial optimization of the TARA geometry based on the variation of two parameters of our IEs: the TARA-reflector shield inclination angle and the shield width. This entailed multiple calculations of MGF functions for electrically large reflectors. Presented in this section is a new formula for computation of the MGF that greatly reduced computation time.

First of all, we introduce some notation. If  $t$  is the integration variable, we will use the cylindrical-coordinate notations of the rotation contour parameterization like  $\rho_0 = \rho_0(t)$ ,  $z_0 = z_0(t)$ ,  $t \in [-1, 1]$ , while for the observation point on the contour of rotation the notations will be  $\rho = \rho(\tau)$ ,  $z = z(\tau)$ ,  $\tau \in [-1, 1]$ . Each integration point on the surface is defined by the parameter  $t$  and the azimuth angle  $\psi$ , and the observation point is defined by the parameters  $\tau$ ,  $\varphi$ .

The MGF is the  $M$ -th term of the Green's function  $\exp(-ikL)/kL$  expansion into the Fourier series in the azimuthal variable. The calculation of the MGF

$$S_M = \int_0^{2\pi} \frac{\exp(-ikL)}{kL} \cos(M\psi) d\psi \quad (11)$$

$$L = \left[ \rho^2 + \rho_0^2 - 2\rho\rho_0 \cos\psi + (z - z_0)^2 \right]^{\frac{1}{2}} \quad (12)$$

and its first and second derivatives is the most time-consuming operation. Here,  $L$  is the distance between the observation point with parameter  $\varphi = 0$  and the integration point with parameters  $\psi$ ,  $t$ .

Changing the integration variable in (11) to

$$u = L(\psi) \quad (13)$$

we arrive at

$$S_M = 4 \int_{L_{\min}}^{L_{\max}} \frac{\exp(-iku) T_M[g(u)]}{k [(u^2 - L_{\min}^2)(L_{\max}^2 - u^2)]^{\frac{1}{2}}} du \quad (14)$$

where  $T_M(x)$  is the Chebyshev polynomial of the first-kind

$$g(u) = [\rho^2 + \rho_0^2 + (z - z_0)^2 - u^2] \cdot (2\rho\rho_0)^{-1}$$

$$L_{\min}^2 = (\rho - \rho_0)^2 + (z - z_0)^2$$

$$L_{\max}^2 = (\rho + \rho_0)^2 + (z - z_0)^2.$$

The calculation of the function  $S_M$  is needed to obtain the values of IE kernels and the near field [14]. In the case of  $t \rightarrow \tau$  (that means  $L_{\min} \rightarrow 0$ ), we have  $S_M \rightarrow \infty$ . This case appears in the IE kernels calculation [14] and they have finite limiting values which can be obtained analytically using the asymptotic behavior of the MGF—see [6] and Appendix. Therefore we are more interested in the case of  $L_{\min} \neq 0$ .

If  $L_{\min} = 0$  then the kernels in the IE have finite limits, which are calculated using the asymptotic behavior of the MGF [6]. Next we consider the case of  $L_{\min} \neq 0$ . Introduce a real function

$$f(u) = \frac{T_M[g(u)]}{k \sqrt{(u + L_{\min})(u + L_{\max})}} \quad (15)$$

then substitute  $u(x) = [L_{\min}(1-x) + L_{\max}(1+x)]/2$  into (14) to obtain the term  $(1-x^2)^{1/2}$  in the denominator of integrand (similarly to the integral representation of the Bessel function that we use in (19) below), and change integration variable to  $\cos(\psi)$ . After this we obtain

$$S_M = 4C \cdot \int_{-1}^1 \frac{\exp(-i\Omega x) f[u(x)]}{\sqrt{1-x^2}} dx \quad (16)$$

where  $C = \exp[-ik(L_{\max} + L_{\min})/2]$ ,  $\Omega = k(L_{\max} - L_{\min})/2$ .

Note that the function  $\tilde{f}(x) = f[u(x)]$  is infinitely differentiable and has only  $M$  oscillations (if CHE is placed on the  $z$  axis then  $M = 1$ ) Therefore it can be interpolated with low order  $f(x) \approx f_{n-1}(x)$ . Any infinitely differentiable function can be expressed in the form of

$$\tilde{f}(x) = \sum_{p=0}^{\infty} a_p T_p(x), \quad x \in [-1, 1] \quad (17)$$

$$a_p = \frac{2 - \delta_{p,0}}{\pi} \int_{-1}^1 \frac{T_p(x) \tilde{f}(x)}{\sqrt{1-x^2}} dx \quad (18)$$

where  $\delta_{p,0} = 1$  if  $p = 0$  and 0 otherwise.

Using the formula [27, 7.355]

$$\int_{-1}^1 e^{-i\Omega x} \frac{T_n(x)}{\sqrt{1-x^2}} dx = \pi(-i)^n J_n(\Omega) \quad (19)$$

and (16), (17) we obtain the expression for the MGF in the form of the series

$$S_M = 4C\pi \sum_{p=0}^{\infty} (-i)^p a_p J_p(\Omega) \quad (20)$$

where  $J_n(x)$  is the Bessel function of order  $n$ .

Because of the infinite differentiability of the function  $f(x)$ , the terms of the series (20) tend to zero with an exponential rate if  $p \rightarrow \infty$ .

Let us evaluate the number of terms we need to calculate in the series (20). To this end, we have to find the polynomial which interpolates the function  $\tilde{f}(x)$  with small enough relative error. Because of the factor  $h = [u + L_{\min}]^{-1/2}$  the function  $f(u)$  in (15) has a large derivative at  $u = L_{\min}$  in the case of  $L_{\min} \rightarrow 0$ . To find the degree of the polynomial which interpolates the factor  $h$  as a function of  $x$ , we obtain it exactly for the mentioned function,

$$\frac{1}{u(x) + L_{\min}} = \sum_{p=0}^{\infty} b_p T_p(x) \quad (21)$$

$$b_p = \frac{2}{\pi} \frac{2}{3L_{\min} + L_{\max}} \int_{-1}^1 \frac{T_p(x)}{(1+ax)\sqrt{1-x^2}} dx, \quad p \geq 1 \quad (22)$$

where  $a = (L_{\max} - L_{\min}) / (3L_{\min} + L_{\max})$ ,  $0 \leq a < 1$ .

Substituting  $x = \cos(\psi)$  in (22) and taking into account [27, 3.613] we have

$$\begin{aligned} b_p &= \frac{2}{\pi} \frac{2}{3L_{\min} + L_{\max}} \int_0^{\pi} \frac{\cos(p\psi)}{1 + a \cos \psi} d\psi \\ &= \frac{4}{3L_{\min} + L_{\max}} \frac{1}{\sqrt{1-a^2}} \left( \frac{\sqrt{1-a^2} - 1}{a} \right)^p \end{aligned} \quad (23)$$

Therefore  $|b_p| < \varepsilon$  if

$$p > \frac{\ln \varepsilon + \ln \left( (3L_{\min} + L_{\max}) \sqrt{1-a^2} - \ln(4) \right)}{\ln \left( \sqrt{1-a^2} - 1 \right) - \ln(a)} = \tilde{N}(\varepsilon) \quad (24)$$

Hence, as function  $f(u(x))$  has  $M$  oscillations, for a sufficiently small error it is necessary to calculate the first  $n = N(\varepsilon) + M$  terms in the series (20), where  $N(\varepsilon)$  is the first integer larger than  $\tilde{N}(\varepsilon)$ . To calculate the coefficients  $a_p$ , we use the quadrature formulas [24]

$$a_p = \frac{2 - \delta_{p,0}}{n} \sum_{m=0}^{n-1} T_p(t_m^n) f_{n-1}(t_m^n) \quad (25)$$

where  $t_p^n = \cos(\pi(2p+1)/2n)$ ,  $p = 0, 1, \dots, n-1$  are the roots of the Chebyshev polynomial of the first kind. Because of the infinite differentiability of the integrand in (18), the quadrature formula (25) has exponential convergence.

Note that  $J_p(\Omega)$  quickly tends to zero if  $p > \Omega$ . Therefore, in the case of certain parameters of the MGF we do not need to calculate all of the first  $n$  items in (20). From [28, 9.1.62] we have

$$|J_m(x)| \leq \frac{\left(\frac{x}{2}\right)^m}{m!} \quad (26)$$

Using the asymptotic expression  $m! \approx \sqrt{2\pi m} (m/e)^m$ , the Bessel function can be approximated as

$$|J_m(x)| \underset{m \rightarrow \infty}{\approx} \frac{1}{\sqrt{2\pi m}} \left(\frac{x \cdot e}{2m}\right)^m. \quad (27)$$

If  $m > xe/2$  then in the right-hand side of (27) we have the powers of the quantity smaller than unity. Numerical ex-

periments show that it is enough to take  $n_1 = \min\{n, m\}$ ,  $m = \Omega e/2 + 5$  terms in (20) for the accuracy of  $10^{-10}$ .

The use of the fast Fourier transform (FFT) can decrease the time required for calculation of  $a_p$  (25). We apply the FFT to calculate

$$\tilde{a} = F_{2n} f_n \quad (28)$$

where  $F_{2n} = \{\exp(-i(pk/2n)2\pi)\}_{p,k=0}^{2n-1}$ ,  $f_n = (f_0, \dots, f_{n-1}, \underbrace{0 \dots 0}_n)$ ,  $\{f_p\}_{p=0}^{n-1} = \{f_{n-1}(t_p^n)\}_{p=0}^{n-1}$ . The coefficients  $a_p$  are expressed through  $\tilde{a}_p$  in the following way:

$$a_p = \text{Re} [\exp(-2\pi i/n) \tilde{a}_p] \cdot (1 + \delta_{p,0})/n \quad (29)$$

The series for the first and the second derivatives of the MGF are derived in an analogous manner. However we need to find the degree of the interpolation polynomial, which approximates the second and the third powers of the factor  $g(x)$ . For this purpose we use the expression [27, 3.613]:

$$\int_0^{\pi} \frac{\cos(n\psi)}{1 - 2a \cos \psi + a^2} d\psi = \frac{\pi a^n}{1 - a^2}, \quad |a| < 1 \quad (30)$$

Note that in the case of small  $L_{\min}$  ( $k \cdot L_{\min} < 2$ ) the series presented in [6, p. 236] converges faster than (20).

Finally, we compare the above mentioned with the approach of [14] to the calculation of MGF. To interpolate the integrand of (11) in [14], we used a trigonometric polynomial. Roughly, the order of this polynomial is proportional to the integrand oscillation number  $n = k \cdot (L_{\max} - L_{\min})/\pi + M$ . For the accuracy  $10^{-6}$  it is enough to set the interpolation order  $5n$ . In the method presented here it is necessary to use the interpolation polynomial for the function  $f(x)$  which has only  $M$  oscillations. Therefore, to have the same accuracy we need to compute  $5k \cdot (L_{\max} - L_{\min})/\pi$  less coefficients of the interpolation polynomial than before, if using the approach of [14]. Thus, quadrature formulas using like in approach [14] requires multiple calculations of MGF functions for electrically large reflectors. The new MGF calculation approach presented in this section has greatly reduced the computation time with the same accuracy.

## V. NEAR AND FAR FIELDS OF THE TARA-LIKE REFLECTOR

### A. Transmission Case

In Fig. 7, the H- and E-plane far-zone radiation patterns of the TARA-like paraboloidal reflector with (red curves) and without (blue curves) conical shield are compared.

One can see that in the direction which is orthogonal to the axis of rotation ( $\theta = 90^\circ$ ), and near to it, the TARA radiation pattern has lower sidelobes than the parabolic reflector alone, by some 20 to 30 dB. The CHE here was taken in such a way that it provided the maximum directivity for the stand-alone paraboloidal reflector.

As one can see, for  $\theta = 90^\circ$  the blue curves differ by some 15 dB from the patterns in Fig. 8 of [3]. This difference can be attributed to the presence of struts and three feed housings in the computations of the patterns in Fig. 8 of [3].

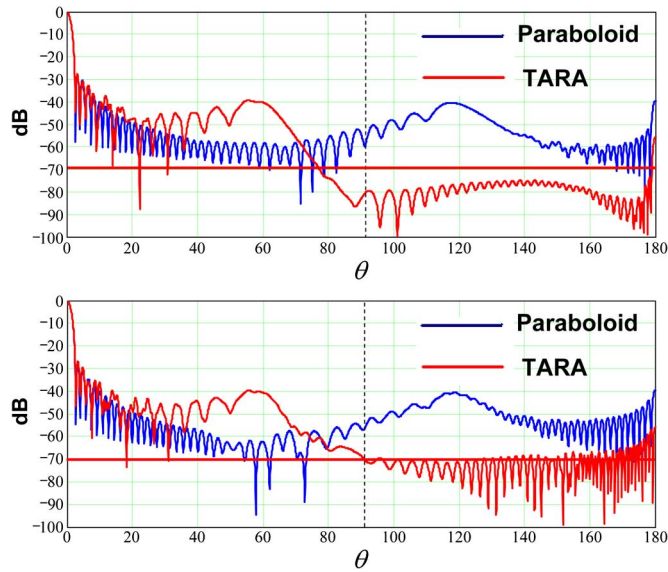


Fig. 7. The total far-zone radiation patterns of the TARA paraboloidal reflector without the conical shield and full TARA-like reflectors illuminated by the optimal CHE, in the H-plane (top) and in the E-plane (bottom).

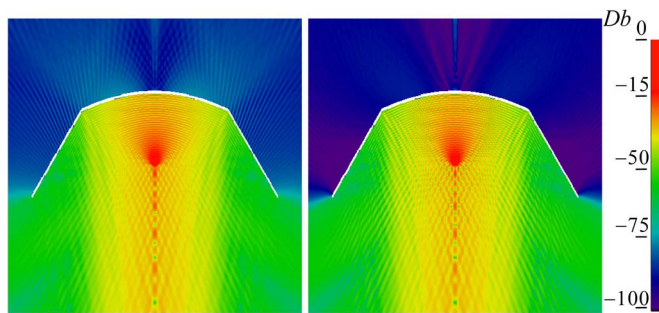


Fig. 8. The near-field of the full TARA-like reflector illuminated by the CHE with the optimal parameter in the H-plane (left) and the E-plane (right).

The calculation time of a far-field pattern is around 100 s on a PC with Intel Core 2 Duo CPU E8400 3.00 GHz and 2 GB of memory. This seems to be several hundred times faster than the code used in [2], [3] (newer versions of that code may reduce this to the factor of 10 [29]).

In Fig. 8 we show, on the logarithmic scale, the near-zone field  $|\vec{E}^{tot}|/|\vec{E}^0|$  of the full TARA fed by the optimal CHE, in the E and H-planes. One can notice a deeper shadow behind the reflector assisted with a shield than in Fig. 6.

### B. Reception Case

In this case, the incident plane electromagnetic wave is assumed to propagate along the  $z$ -axis direction. It is interesting to compare the near fields  $|\vec{E}^{tot}|/|\vec{E}^0|$  of the stand-alone paraboloidal reflector (Fig. 9) and the full TARA-like reflector (Fig. 10).

In Fig. 10 we can see an interesting phenomenon that has escaped geometrical-optics descriptions and the MLFMA-MM simulations in [2], [3].

In addition to the main focal spot (area of the field concentration), there is another parasitic “focus” near the paraboloid vertex, split into two bright spots in the H-plane.

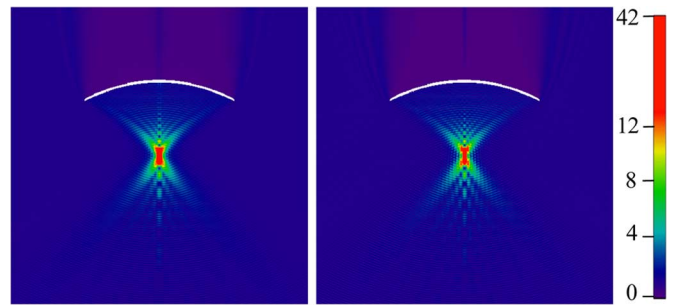


Fig. 9. The near-field of the TARA-like stand-alone paraboloidal reflector illuminated by the on-axis plane wave in the H-plane (left) and the E-plane (right).

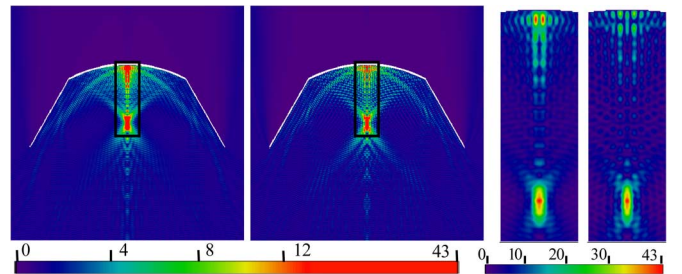


Fig. 10. The near-field of the TARA-like shielded reflector illuminated by the on-axis plane wave in the H-plane (the first plot at the left) and the E-plane (the second plot), the field inside the black rectangle in the H-plane (the third plot) and the E-plane (the fourth plot).

These areas of additional field concentration appear because of specular reflection of incoming wave by the upper part of the conical shield that directs the wave to the vertex of paraboloid (we are grateful to the associate editor for this observation). These simple geometrical considerations help, in part, explain the shape of the mentioned areas. The distance from the split focus to the geometric focus of paraboloid and to its vertex is  $15.51\lambda$  and  $0.99\lambda$ , respectively.

Out of curiosity, we have placed the HE between the two split foci locations and compared the far-fields of the TARA-like shield-assisted paraboloidal reflector and a stand-alone paraboloidal reflector illuminated by such a feed—see Fig. 11. It can be seen that a paraboloid without the shield does not produce any reasonable main beam with the feed at that point.

In contrast, the shield-assisted paraboloid fed by a HE placed between the split parasitic foci radiates a sort of conical beam with a minimum in the direction of the  $z$ -axis.

### C. Elementary Optimization

An interesting question is whether the TARA antenna characteristics can be preserved or improved if the width of the conical shield is reduced, possibly for a different value of its inclination angle  $\theta_0$ . Such optimization may seem elementary (only two control parameters are involved) however, to be successful with the 80-wavelength reflector, it needs an accurate and economic computational instrument. The IE-Nystrom algorithm of [14] combined with the approach presented in Section IV meets this requirement.

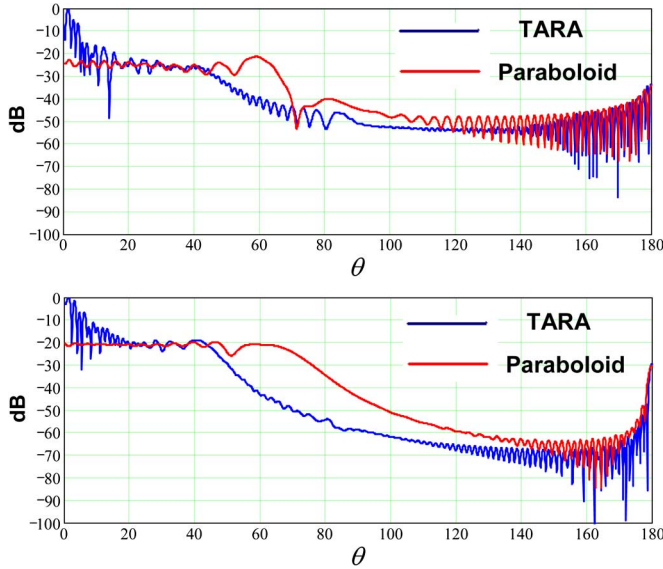


Fig. 11. The total far-zone radiation patterns of the shielded paraboloidal and stand-alone paraboloidal reflector illuminated by a conventional HE placed in the parasitic focus location in the H-plane (top) and in the E-plane (bottom).

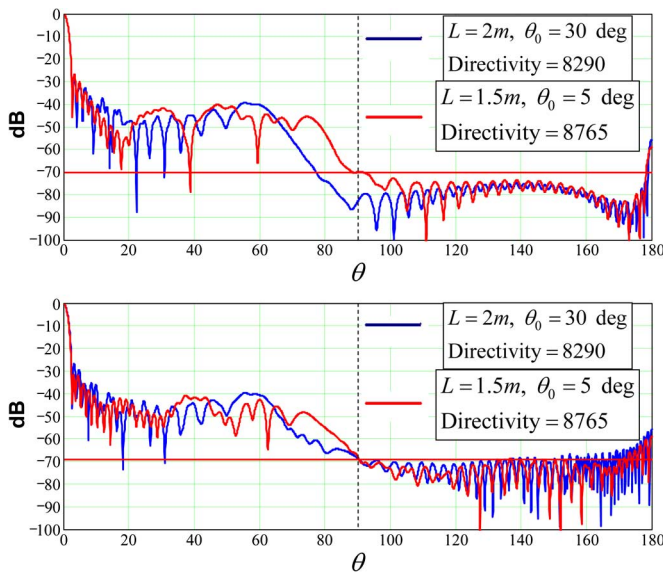


Fig. 12. The total far-zone radiation patterns of the in-focus CHE fed TARA-like reflector in the H-plane (top) and in the E-plane (bottom) for  $\varphi_0 = 5^\circ$ ,  $L = 1.5$  m and  $\varphi_0 = 30^\circ$ ,  $L = 2$  m.

As an outcome of this optimization, in Fig. 12, we compare the far-field patterns of a shield-assisted reflector with  $\theta_0 = 5^\circ$  and  $l = 1.5$  m and of the real TARA ( $\theta_0 = 30^\circ$ ,  $l = 2$  m).

Comparison shows that the shield-assisted paraboloidal reflector with  $\theta_0 = 5^\circ$  and  $l = 1.5$  m satisfies the major antenna design requirement on the sidelobes referred to above. It should be noted that the directivity of such a modified reflector is even larger than for the actual TARA.

## VI. CONCLUSIONS

We have introduced important improvements to the algorithm initially presented in [12]–[14] enabling more efficient analysis of rotationally symmetric reflector antennas of quasi-optical size. For this purpose we have derived a new series form for

the MGF. The terms of the series tend to zero with exponential rate and calculation time does not depend on the electrical size of reflector. Using such series we have been able to investigate an electrically large TARA-like shield-assisted paraboloidal reflector antenna on a PC.

To model the TARA feed we have used a CHE with an optimal aperture-size parameter. For a CHE located on the axis one needs to solve only one set of a 1-D hypersingular and a singular IE. This system corresponds to the first azimuthal harmonic of the current density components.

We have considered the far-field of the TARA-like antenna in the transmission case and found that the calculation time is hundreds times smaller than with the MLFMA-MM algorithm of [2], [3] although this advantage can reduce to 10 with newer versions [29]. In the on-axis reception case, an interesting physical effect has been observed that escapes geometrical-optics descriptions: in addition to the main focal spot (area of field concentration), there is another parasitic “focus” near the paraboloid vertex, split to two spots in the H-plane.

Thanks to the high efficiency of computations, elementary numerical optimization of the TARA-like paraboloid-plus-shield antenna has been performed. We have shown that the directivity can be improved, and the width of the conical shield can be reduced by a half meter, by changing the shield inclination from  $30^\circ$  to  $5^\circ$ .

The use of the rigorous theory of integral equations with a Nystrom-type discretization offers many opportunities, not only in reflector antenna design. For instance, one can find numerous applications in the electromagnetic diffraction and eigenvalue problems for dielectric bodies. This can be a direction of further research.

## APPENDIX

In Section IV we have considered how to compute MGF (11), (12) in the case of the integration variable  $t$  not equal to the observation point  $\tau$ . Here we show what happens if  $\tau \rightarrow t$  in IE kernels, which contain MGF.

All kernels given by (33)–(36) of [14] in IE (28) of [14] are smooth (belong to the Holder space  $C^{1,\alpha}$ ,  $\alpha < 1$ ) and of course have finite limits,  $K(\tau, t) \rightarrow K(t)$  if  $\tau \rightarrow t$ . The limits of IE kernels can be derived analytically using asymptotic behavior of MGF  $S_M$  as it had been described in [6]. Because of complexity of this derivation we do not represent all these limits here. For a rough calculation it is possible to obtain this values numerically as  $K(t) = K(t + \varepsilon, t)$ , where  $\varepsilon > 0$  is a “small” number, for example  $\varepsilon = 10^{-6}$ .

As an example, now we consider the limit for the kernel  $K_{22}^M(\tau, t) = \rho^3[(M^2/\rho)S_M - k^2\rho_0 S_M^+] - c_{22}^M(\tau) \ln |\tau - t|$  (see (36) in [14]). This is the simplest of all kernels and therefore it does not need huge space for derivation. At first consider the asymptotic behavior of MGF

$$S_M(\tau, t) = \int_0^{2\pi} (e^{-ikL} \cos(M\psi) - 1) \cdot L^{-1} d\psi + \int_0^{2\pi} L^{-1} d\psi. \quad (\text{A1})$$

Denote the smooth first term at the right-hand part of (A1) as

$$Q_M(\tau, t) = \int_0^{2\pi} (e^{-ikL} \cos(M\psi) - 1) L^{-1} d\psi. \quad (\text{A2})$$

It is possible to show that

$$\int_0^{2\pi} \frac{1}{L} d\psi = \frac{4K(\nu)}{r^*} \quad (\text{A3})$$

where  $K(\nu)$  is the complete elliptic integral of the first kind,

$$r^* = r^*(\tau, t) = \sqrt{(\rho + \rho_0)^2 + (z - z_0)^2} \quad (\text{A4})$$

$$\nu = \nu(\tau, t) = \frac{2\sqrt{\rho \cdot \rho_0}}{r^*}. \quad (\text{A5})$$

In [27] and [28] the following asymptotic behavior is given:

$$K(\nu) \underset{\nu \rightarrow 1}{=} \ln \left[ \frac{4}{(1-\nu^2)} \right] + \left( \frac{1}{4} \right) (1-\nu^2) \left\{ \ln \left[ \frac{4}{(1-\nu^2)} \right] - 1 \right\} + O \left[ (1-\nu^2)^2 \ln(1-\nu^2) \right]. \quad (\text{A6})$$

Using (A3) and (A6) we see that the singular second term in (A1) behaves as

$$\int_0^{2\pi} \frac{d\psi}{L} \underset{t \rightarrow \tau}{=} -\frac{2}{\rho} \ln |\tau - t| + \frac{2}{\rho} \ln \frac{8\rho}{\sqrt{\rho'^2 + z'^2}} + O \left[ (t - \tau) \ln |\tau - t| \right], \quad (\text{A7})$$

where a prime means differentiation with respect to variable  $t$ .

Therefore, from (A7) and (A2) we obtain the following result:

$$\lim_{\tau \rightarrow t} \left[ S_M + \frac{2}{\rho} \ln |\tau - t| \right] = Q_M(t, t) + \frac{2}{\rho} \ln \frac{8\rho}{\sqrt{\rho'^2 + z'^2}}. \quad (\text{A8})$$

From (A2) we can also find that

$$Q_M(t, t) = 2 \int_0^{\pi} \frac{\exp \left( -ik\rho(t) 2 \sin \left( \frac{\psi}{2} \right) \right) \cos(M\psi) - 1}{k\rho(t) 2 \sin \left( \frac{\psi}{2} \right)} d\psi. \quad (\text{A9})$$

Finally, using (A7) we obtain the expression that we have been looking for

$$K_{22}^M(t, t) = \rho(t)^3 \left\{ \frac{2}{\rho(t)} \ln \frac{8\rho(t)}{\sqrt{\rho'(t)^2 + z'(t)^2}} \left[ \frac{M^2}{\rho(t)} - k^2 \rho(t) \right] + \frac{M^2}{\rho(t)} Q_M(t, t) - \frac{k^2 \rho(t)}{2} [Q_{M-1}(t, t) + Q_{M+1}(t, t)] \right\} \quad (\text{A10}).$$

Similar treatment of  $\lim_{\tau \rightarrow t} K_{11}^M(\tau, t)$  takes several pages and therefore we do not show this bulky derivation in the paper.

#### REFERENCES

- [1] [Online]. Available: <http://home.tudelft.nl/en/research/knowledge-centres/ircrtr/research/radar/research-facilities/tara/>
- [2] A. Heldring, "Full Wave Analysis of Electrically Large Reflector Antennas," Ph.D. dissertation, Delft Univ. Press, Delft, The Netherlands, 2002.
- [3] A. Heldring, J. M. Rius, L. P. Ligthart, and A. Cardama, "Accurate numerical modeling of the TARA reflector system," *IEEE Trans. Antennas Propag.*, vol. 52, no. 7, pp. 1758–1766, 2004.
- [4] S. M. Rao, D. R. Wilton, and A. W. Glisson, "Electromagnetic scattering by surfaces of arbitrary shape," *IEEE Trans. Antennas Propag.*, vol. 30, no. 3, pp. 409–418, 1982.
- [5] A. G. Davydov, E. V. Zakharov, and Y. V. Pimenov, "Numerical decision method of the electromagnetic wave diffraction by unclosed surfaces problem," *Dokl. Akad. Nauk SSSR*, vol. 276, no. 1, pp. 96–100, 1984.
- [6] E. N. Vasilyev, *Excitation of Bodies of Rotation* (in Russian). Moscow, Russia: Radio i Svyaz, 1987.
- [7] A. Berthon and R. Bills, "Integral analysis of radiating structures of revolution," *IEEE Trans. Antennas Propag.*, vol. 37, no. 3, pp. 159–170, 1989.
- [8] A. G. Davydov, E. V. Zakharov, and Y. V. Pimenov, "Numerical analysis of fields in the case of electromagnetic excitation of unclosed surfaces," *J. Commun. Technol. Electron.*, vol. 45, pp. S247–S259, 2000, Supp. 1.2.
- [9] A. A. Nosich, Y. V. Gandel, T. Magath, and A. Altintas, "Numerical analysis and synthesis of 2-D quasi-optical reflectors and beam waveguides based on an integral-equation approach with Nystrom's discretization," *J. Opt. Soc. Amer. A*, vol. 24, no. 9, pp. 2831–2836, 2007.
- [10] J. L. Tsalamengas, "Exponentially converging Nystrom methods in scattering from infinite curved smooth strips. Part 1: TM-Case," *IEEE Trans. Antennas Propag.*, vol. 58, no. 10, pp. 3265–3274, 2010.
- [11] J. L. Tsalamengas, "Exponentially converging Nystrom methods in scattering from infinite curved smooth strips. Part 2: TE-case," *IEEE Trans. Antennas Propag.*, vol. 58, no. 10, pp. 3275–3281, 2010.
- [12] M. V. Balaban, E. I. Smotrova, O. V. Shapoval, V. S. Bulygin, and A. I. Nosich, "Nystrom-type techniques for solving electromagnetics integral equations with smooth and singular kernels," *J. Numerical Modeling: Electron. Networks, Devices Fields*, vol. 25, no. 5, pp. 490–511, 2012.
- [13] V. S. Bulygin, Y. V. Gandel, and A. I. Nosich, "Near field focusing and radar cross section for a finite paraboloidal screen," in *Proc. Eur. Conf. Antennas Propag. (EuCAP-2011)*, 2011, pp. 3678–3682.
- [14] V. S. Bulygin, A. I. Nosich, and Y. V. Gandel, "Nystrom-type method in three-dimensional electromagnetic diffraction by a finite PEC rotationally symmetric surface," *IEEE Trans. Antennas Propag.*, vol. 60, no. 10, pp. 4710–4718, 2012.
- [15] M. R. Barclay and W. V. T. Rusch, "Moment-method analysis of large, axially symmetric reflector antennas using entire-domain functions," *IEEE Trans. Antennas Propag.*, vol. 39, no. 4, pp. 491–496, 1991.
- [16] W. Gander and W. Gautschi, "Adaptive quadrature-revisited," *BIT Numer. Mat.*, vol. 40, no. 1, pp. 84–101, 2000.
- [17] A. A. K. Mohsen and A. K. Abdelmageed, "A fast algorithm for treating EM scattering by bodies of revolution," *Int. J. Elect. Commun.*, no. 3, pp. 164–170, 2001.
- [18] K. Abdelmageed, "Efficient evaluation of modal Green's functions arising in EM scattering by bodies of revolution," *Prog. Electromagn. Res.*, vol. 27, pp. 337–356, 2000.
- [19] R. D. Graglia, P. L. E. Uslenghi, R. Vitiello, and U. D'Elia, "Electromagnetic scattering for oblique incidence on impedance bodies of revolution," *IEEE Trans. Antennas Propag.*, vol. 43, pp. 11–26, 1995.
- [20] W. M. Yu, D. G. Fang, and T. J. Cui, "Closed form modal Green's functions for accelerated computation of bodies of revolution," *IEEE Trans. Antennas Propag.*, vol. 56, no. 11, pp. 3452–3461, 2008.
- [21] D. R. Wilton and N. J. Champagne, "Evaluation and integration of the thin wire kernel," *IEEE Trans. Antennas Propag.*, vol. 54, no. 4, pp. 1200–1206, 2006.
- [22] D. Greenwood and J.-M. Jin, "Finite-element analysis of complex axisymmetric radiating structures," *IEEE Trans. Antennas Propag.*, vol. 47, no. 8, pp. 1260–1266, 1999.
- [23] S. D. Gedney and R. Mittra, "The use of the FFT for the efficient solution of the problem of electromagnetic scattering by a body of revolution," *IEEE Trans. Antennas Propag.*, vol. 38, no. 3, pp. 313–322, 1990.
- [24] Y. V. Gandel, *Introduction to the Methods of Computation of Singular and Hypersingular Integrals* (in Russian). Kharkiv, Russia: Kharkiv Nat. Univ. Press, 2001.
- [25] Y. V. Gandel, S. V. Eremenko, and T. S. Polyanskaya, *Mathematical Problems of the Method of Discrete Currents* (in Russian). Kharkiv: Kharkiv Nat. Univ. Press, 1992.
- [26] Y. V. Gandel and A. S. Kononenko, "Justification of the numerical solution of a hypersingular integral equation," *Differential Equations*, vol. 42, no. 9, pp. 1326–1333, 2006.

- [27] I. S. Gradshteyn and I. M. Ryzhik, *Table of Integrals, Series, and Products*. New York, NY, USA: Academic, 1994.
- [28] M. Abramowitz and I. A. Stegun, *Handbook of Mathematical Functions*, National Bureau of Standards Applied Mathematics Series 1964.
- [29] J. M. Rius, private communication.



**Vitaliy S. Bulygin** (M'09) was born in 1985 in Kharkiv, Ukraine. He received the M.S. degree in mathematical modelling from the Kharkiv National University, Kharkiv, Ukraine, in 2007 and the Ph.D. degree from the Institute of Problems of Machine Engineering, National Academy of Sciences of Ukraine (NASU), in 2010.

Since 2010 he has been with the Institute of Radio-Physics and Electronics NASU in Kharkiv. His research interests are in integral equations, numerical methods, antennas, and electromagnetic

wave diffraction.

Dr. Bulygin won the N. I. Akhiezer Fellowship in 2009 and the Best Young Scientist Paper Prize of the European Microwave Association at the MSMW-10 international symposium in Kharkiv in 2010. In 2012, he was a recipient of the mobility grant of the European Science Foundation Research Networking Programme "Newfocus."



**Trevor M. Benson** (M'95–SM'01) received the degree (first class hon) in physics and the Clark Prize in experimental physics and the Ph.D. degree in electronic and electrical engineering from the University of Sheffield, Sheffield, U.K., in 1979 and 1982, respectively, and the D.Sc. degree from the University of Nottingham, Nottingham, U.K., in 2005.

After spending over six years as a Lecturer at the University College Cardiff, he moved to the University of Nottingham in 1989. He was promoted to a Chair in Optoelectronics in 1996, having previously been Senior Lecturer (1989) and Reader (1994). Since October 2011, he has been Director of the George Green Institute for Electromagnetics Research at The University of Nottingham. His research interests include experimental and numerical studies of electromagnetic fields and waves with particular emphasis on the theory, modeling and simulation of optical waveguides, lasers and amplifiers, nano-scale photonic circuits and electromagnetic compatibility.

Prof. Benson is a Fellow of the Institute of Engineering Technology (FIET) and the Institute of Physics (FInst.P). He was elected a Fellow of the Royal

Academy of Engineering in 2005 for his achievements in the development of versatile design software used to analyze propagation in optoelectronic waveguides and photonic integrated circuits.



**Yuriy V. Gandel** (M'02–SM'04) was born in Kharkiv, Ukraine, in 1934. He received the M.S. and Ph.D. degrees in mathematical physics and the D.Sc. degree in radio physics from the Kharkiv National University, Kharkiv, Ukraine, in 1962, 1971, and 1994, respectively.

Since 1995, he has been a Professor of mathematical physics at the Kharkiv National University. His research interests are in singular and hypersingular integral equations, numerical methods, and modeling of electromagnetic and acoustic wave scattering by

screens and gratings.

Dr. Gandel was awarded the honorary medals of "Distinguished Teacher of Ukraine" and "Distinguished Educator of Ukraine" in 1967 and 2005, respectively, and an N. I. Akhiezer Fellowship in 2005. He was the co-recipient the Best Paper Award of the ISAP'04 International Symposium in Sendai, Japan, in 2004.



**Alexander I. Nosich** (M'94–SM'95–F'04) was born in 1953 in Kharkiv, Ukraine. He received the M.S., Ph.D., and D.Sc. degrees in radio physics from the Kharkiv National University, Ukraine, in 1975, 1979, and 1990, respectively.

Since 1979, he has been with the Institute of Radio Physics and Electronics of the National Academy of Science of Ukraine, Kharkiv, where he is currently Professor and Principal Scientist heading the Laboratory of Micro and Nano-Optics. Since 1992, he has held a number of guest fellowship and professorship in the EU, Japan, Singapore, and Turkey. His research interests include the method of analytical regularization, propagation and scattering of waves, open waveguides, antennas and lasers, and the history of microwaves.

Prof. Nosich was one of the initiators and Technical Committee Chairman of the International Conference Series on Mathematical Methods in Electromagnetic Theory (MMET). In 1995, he organized IEEE AP-S East Ukraine Chapter, the first one in the former USSR. Currently he represents Ukraine, Georgia, and Moldova in the European Association on Antennas and Propagation.